

Article

Not peer-reviewed version

---

# 3D Printing with Earthen Materials: A Settlement-Scale Design Experience

---

[Leonardo Giacomobono](#) , [Maria Argenti](#) , [Elena Ferretti](#) <sup>\*</sup> , [Giulio Paparella](#) <sup>\*</sup>

Posted Date: 5 August 2024

doi: 10.20944/preprints202408.0259.v1

Keywords: Digitization; 3D Printing; Earth; Housing System; Settlement; Automation



Preprints.org is a free multidiscipline platform providing preprint service that is dedicated to making early versions of research outputs permanently available and citable. Preprints posted at Preprints.org appear in Web of Science, Crossref, Google Scholar, Scilit, Europe PMC.

Copyright: This is an open access article distributed under the Creative Commons Attribution License which permits unrestricted use, distribution, and reproduction in any medium, provided the original work is properly cited.

Article

# 3D Printing with Earthen Materials: A Settlement-Scale Design Experience

Leonardo Giacomobono <sup>1</sup>, Maria Argenti <sup>2</sup>, Elena Ferretti <sup>3,\*</sup> and Giulio Paparella <sup>4,\*</sup>

<sup>1</sup> giacomobono.1798299@studenti.uniroma1.it

<sup>2</sup> maria.argenti@uniroma1.it

<sup>3</sup> elena.ferretti2@unibo.it

<sup>4</sup> giulio.paparella@uniroma1.it

\* Correspondence: elena.ferretti2@unibo.it (E.F.); giulio.paparella@uniroma1.it (G.P.)

**Abstract:** The research theme originates as a design experiment for a sustainable housing system built on-site. The context is Niamey, the capital of Niger. The study takes into account the environmental issues in the construction sector and aims to find a solution capable of meeting housing, environmental, and economic needs. In the field of earthen construction, the most important developments have been achieved in manufacturing methods. In particular, the use of an additive digital manufacturing system, such as large-scale 3D printing, allows the construction of complex shapes derived from structural and thermal studies, maintaining a high degree of automation in the construction process, reducing construction times and labor costs. The research investigates the possibility of responding to housing and environmental needs with a settlement system made entirely of printed earth, maintaining the highest possible degree of automation. Starting from a study on the state of the art of 3D printing in architecture and printable earthen compounds, the design choices of similar cases are analyzed to understand the construction techniques, potentials, and limitations of the medium. Finally, a design proposal is developed based on the definition of a fully printable functional module, which, upon aggregation, determines the characteristics of the final settlement.

**Keywords:** digitization; 3D printing; earth; housing system; settlement; automation

## 1. Introduction

In recent times, the progressive digitization of design and execution tools for architecture seems to open new opportunities that can significantly contribute to the increasingly urgent environmental, social, and economic issues [1].

Among the different construction technologies, large-scale 3D printing allows for the direct on-site creation of customized architectural solutions, even for residential purposes, optimizing the use of resources and raw materials [2]. Among the possible digital additive construction processes, the approach of direct 3D printing with earthen-based compounds seems to offer a viable sustainable alternative to the use of concrete, which is widely adopted in conventional constructions but highly impactful from an environmental perspective. Suffice it to say that concrete is responsible for 8% of global carbon dioxide (CO<sub>2</sub>) emissions (concrete carbon footprint) [3], 90% of which are due to the production of clinker, which is the main ingredient that gives concrete strength. For this reason, the Paris Climate Agreement stipulated that the global concrete industry must reduce emissions by 25% per m<sup>3</sup> of concrete by 2030, and 100% by 2050 to stay within the 1.5°C warming carbon budget [4]. Therefore, reducing the demand for carbon-intensive clinkers with new techniques and new ingredients is an imperative that poses a great challenge to researchers in the construction industry. In this perspective, the present article offers an overview of the limitations and application potentials of large-scale direct 3D printing with earthen compounds, associated with the use of computational-parametric design tools, for the realization of sustainable housing systems.

The work presents multiple objectives, tools, and methods, and sees in the coordination capacity of the architectural project an opportunity to support the entire methodological framework. Oriented towards reducing the time and emissions due to production, transportation, and assembly, the design

of the earthen housing system focuses both on the possibility of on-site production and on achieving a high level of automation in the construction process through the much sought-after 'wall-roof continuity'. The design choice which allowed us to cope with the mechanical properties of the earthen material (a compression-resistant material) and avoid the use of temporary works, was to recover ancient construction techniques based on the funicular of loads. From the point of view of the construction technique, this involved the use of robotic arms capable of depositing material on non-horizontal planes.

The work began with the definition of a fully printable functional module. The two construction elements were then studied, roof and vertical closure, in order to ensure the stability of the module both during the realization phase and once construction is completed. The validity of the system was subsequently verified by designing a possible application.

### *1.1. Premises on Environmental Sustainability*

Human activity over the centuries has significantly impacted current environmental conditions. According to the "2022 Global Climate Highlights," 2022 was the second warmest year on record in Europe and the fifth warmest globally. It has been recorded that the average annual temperatures have risen by 0.3 degrees compared to the reference period (1991-2020), and by 1.2 degrees compared to the pre-industrial period (1850-1900) [5]. This makes 2022 the eighth consecutive year in which the average annual temperatures exceed the pre-industrial period temperatures by one degree. These temperatures have caused environmental upheavals and damaging phenomena across the globe. It is therefore crucial to halt the temperature increase before reaching an average annual increase of two degrees compared to the pre-industrial level, a temperature beyond which we will face irreversible effects on the environment.

It is commonly believed that the increase in average temperatures is due to the constant rise in the amount of CO<sub>2</sub> released into the atmosphere. Although global CO<sub>2</sub> levels are slightly decreasing, the entire construction sector contributes 38% to the amount of carbon dioxide emitted [5]. Current directives aim at the construction of NZEB (Near Zero Emission Building), buildings with very high energy performance, whose energy needs are very low and almost entirely covered by renewable energy sources. However, 10% of global emissions are due to the production, transportation, and subsequent disposal of construction materials. It follows that we must act not only on the energy impact that the building has during its life but also on the construction materials, employing construction systems whose production releases less CO<sub>2</sub> into the environment, are easily disposable, and minimize transportation between the factory and the construction site.

### *1.2. Building with Earth*

Regarding earthen compounds, it should be emphasized that the novelty does not lie in the material itself, but in the fabrication method used to construct the buildings.

The use of earth as a building material offers numerous advantages: it is recyclable, easily available, and inexhaustible, it is not harmful, has decent compressive strength, and excellent hygrothermal properties. The porous nature of the material indeed results in the ability to absorb and release moisture, ensuring stable temperatures throughout the year [6]. If properly designed, an earthen wall acts as a passive thermal regulator, further reducing the use of energy for active conditioning systems. Earthen constructions also have a positive effect on increasing the resilience of cities, helping to reduce heat islands [7].

Why don't we build with earth then? Despite the numerous advantages, the choice to construct a new building with earth is extremely unusual; because, depending on the cultural context, such a solution is still considered unconventional or primitive. As a consequence unlike other materials such as reinforced concrete, earth has not reached an adequate level of experimentation that allows it to have an international standard. Therefore, the lack of experimentation results in a lack of reliable data regarding the variations in mechanical and hygrometric characteristics based on different soil types, uncertainty about the various possibilities of reinforcing structural elements, and a lack of effective

quality controls on constructions. The construction times for earthen buildings are also higher compared to industrialized systems.

### 1.3. 3D Printing with Earth: The Challenge of Roofing

Currently, experiments on buildings made with 3D printing in earthen compounds are still limited compared to those involving the use of printed concrete. These case studies can be analyzed through different parameters; our specific focus is on the use of earth for structural purposes. As with traditional earthen constructions, in this case too, it is possible to distinguish two main construction principles: global 3D printing and 3D printing for hybrid construction systems. While a global approach involves the continuous printing of the entire building through the wall-roof continuity, the hybrid type involves the printing of vertical elements, which may or may not be load-bearing, combined with the use of roofs made with traditional construction methods and materials [8]. The challenge of gravity, even more crucial in the case of additive construction processes, has suggested the experimentation of hybrid construction approaches in which the roof, generally made of wood, is assembled after the printing of the perimeter walls and lay on them (Figure 1a). Differently, in the Gaia prototype (Figure 1b), created in 2018 by WASP in Massa Lombarda (RA, Italy), they rest directly on an alternative vertical structure [9]. The only global approach realized so far is Tecla (Figure 1c), a unique experiment of its kind, composed of two modules (night area and day area), entirely made of load-bearing printed earth. On the roof, there is a skylight capable of providing illumination to the interior spaces. During the printing phase, some of the interior furnishings are also integrated, in order to speed up the time in which the house becomes available [10].

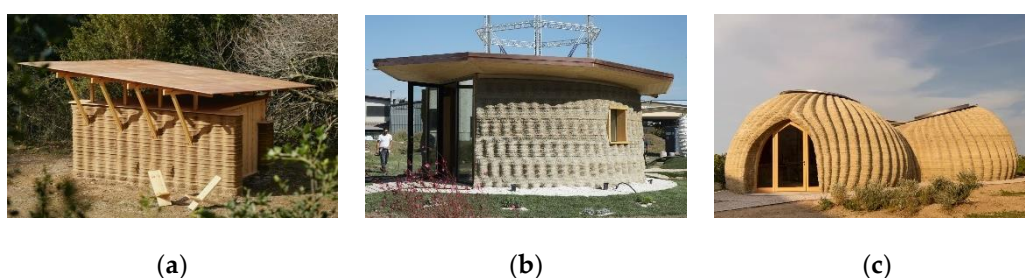


Figure 1. (a) Tova [11]; (b) Gaia [12]; (c) Tecla [13].

## 2. Materials and Methods

### 2.1. Definition of the Project Concept

The functional module is designed to be realized through direct printing with a global approach, the elements are printed on-site and do not need further processing to meet the required performance. In this way, the automation of the construction process is maximized, reducing construction times and pollution due to the assembly and transportation of materials. The construction elements designed are self-supporting and do not require the installation of additional supports.

The designed module (Figure 2) involves the definition of square-plan spaces, covered by a vaulted element. The printing strategy differs for the two construction elements. The wall layers are deposited along horizontal planes (Figure 3a), while the roof is printed along a diagonal by tilting the printing plane by  $45^\circ$  (Figure 3b, 3c). In this way, the layers forming the vault are always deposited on the underlying layer; during printing phase, they have form resistance due to the creation of curved elements subject only to compression.

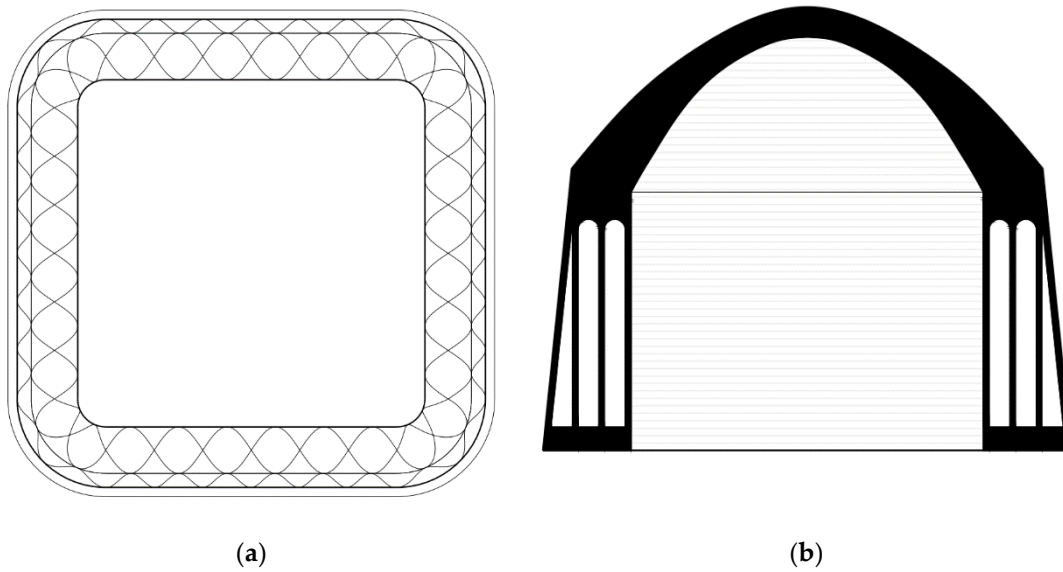


**Figure 2.** (a) Plan of the module; (b) Section of the module.

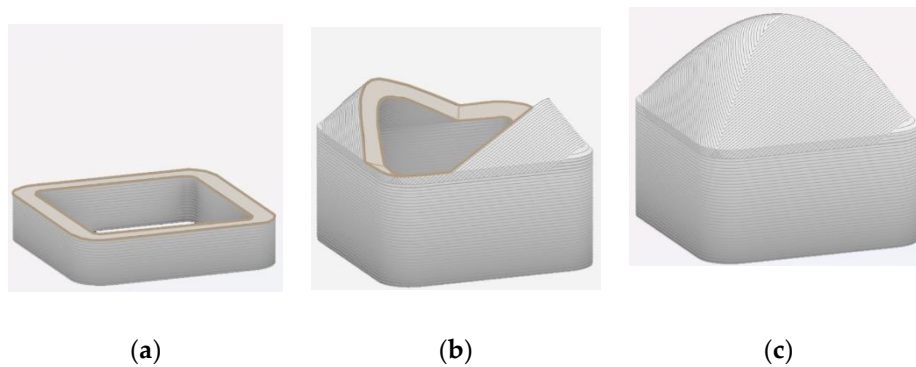


**Figure 3.** (a) Printing on horizontal layers; (b) Printing on 45° inclined layers along the module's diagonal; (c) Completed module.

The printing process adopted derives from traditional Nubian vaults (Figure 4a), which are self-supporting vaults, meaning they can be constructed without any external support during the building phase. This characteristic is due to the inclination at which the rows of bricks are placed. Cutting the vault according to inclined planes and arranging the bricks along these planes ensures that the laid elements always rest on those previously placed [11]. The same principle is adopted and adapted through 3D printing. Prototypes of vaults have already been created using this process (Figure 4b) demonstrating how the inclination of the printing plane allows for an increase in the maximum printing inclination up to 60°.



(a)



(b)

**Figure 4.** (a) Nubian vault [14]; (b) Prototype of a vault printed with 40° inclined layers without supports [15].

Contrary to traditional horizontal slicing, in this case, the extruder, when printing a layer, moves simultaneously on the three axes  $x$ ,  $y$ , and  $z$ , having to remain always perpendicular to the printing plane. This printing strategy therefore involves the use of robotic arms, which possess an extruder with 6 degrees of freedom and allow greater construction flexibility due to their ease of movement compared to framed systems.

## 2.2. Structural Design

The study of the structural design of the module was divided into two parts: the first concerning the analysis of the loads produced by the roof, and the second concerning the design of the wall based on the acting loads. First of all, the study on the mechanical characteristics and composition of the hypothesized compound (Tables 1 and 2) is reported, based on the reference study [16] by Mohamed Gomaa.

### 2.2.1. The Mechanical Properties of the Printed Material

The mix design of the printed compound is similar to a traditional cob mixture, with an increased percentage of water to ensure printability (Table 1). Natural fibres must be in the range of length of 30-50mm in order to ensure the correct extrusion of the material by the printer, they have a beneficial effect on enhancing the compressive strength of the mixture and on reducing the shrinkage of the printed elements. All the reported values, except for the characteristic tensile strength, derive from axial compression tests on printed specimens [16]. For the characteristic tensile strength, average strength values of raw earth walls were used [17], due to the lack of data in this regard. This assumption was possible because the research shows that the mechanical characteristics of the printed specimen are in line with those of a traditional earthen specimen [18], and therefore the printing process does not affect the strengths (Table 2). We can summarize by saying that the material has a brittle behavior, works in compression, and does not have significant tensile strengths. It has lower strengths compared to traditional construction materials, which results in greater thicknesses of the structural elements.

**Table 1.** Mix design of the printed compound [4,5].

<b>Materiale</b>	<b>Percentage by weight</b>
Soil	73%
Water	25%
Wheat fibers (30-50mm)	2%

Table 2. Properties of the compound.

Property	Strength value
Elastic modulus (E)	22.9 MPa
Characteristic compressive strength ( $F_c'$ )	0.62 MPa
Characteristic tensile strength ( $F'_{vk0}$ )	0.24 MPa
Density ( $\gamma$ )	18 KN/m <sup>3</sup>
Poisson's ratio ( $\nu$ )	0.22

### 2.2.2. Roof

Three modules of different sizes have been defined: 4, 9, 12 sqm, and the roof has been designed for each of them. The shape of the vault is generated through Grasshopper, writing an algorithm that simulates an elastic membrane subject to its own weight. In this way, the roof is subjected to compression only.

The preliminary design of the roof was carried out through 3 checks: verification of the pressure curve passing within the middle third of the section, verification of the stresses at the keystone section, and verification of the stresses at the impost section.

#### 2.2.2.1. 12 sqm Block

The verification of the pressure curve was carried out using a graphical method. Considering the midline of the vault in its vertical plane (Figure 5a). This midline was divided into 8 fictitious arches of 1 meter in length, for which the weights of the respective vault segments were calculated (Table 3). The weight vectors are applied to the centroids of the vault segments, which belong to the previously defined arches. Then, the force line is drawn (line where the sum of the forces are applied) and the funicular polygon is constructed. To comply with the graphic rules for finding the resultant vector between incident vectors of the plane, the line of force - which is a vertical line - passes through the intersection point between the first and last sides of the polygon (Figure 5b). At this point, the line orthogonal to the key section applied into the upper third intersects the line  $r'$  at a point C, giving us the line of action of the horizontal force. The line connecting the pole C and the lower third middle of the section at the impost gives us the line of action of the load at the impost. The line of forces has been decomposed according to the horizontal direction and the direction of the line of action at the impost. In this way, it was possible to derive the value of the horizontal force (S) at the keystone and the value of the total load (H) at the impost. Using point C as the projection pole, the pressure polygon was traced and its containment within the middle third of the arch was verified.

Subsequently, an analysis on the stress state of the roof was carried out, in particular, the two sections at the keystone and at the impost were verified. For the first, a bending compression check was carried out, since the pressure curve coincides with the upper middle third and is orthogonal to the plane of the studied section, the pressure will be of bending compression with a triangular diagram. As for the section at the impost, a bending compression and shear check was carried out, as the load is not orthogonal to the plane of the impost. For both verifications, it was verified that the applied stress was less than the design stress. The method used is the same as for the verification of masonry vaults, as these exhibit similarities in behavior. It is indeed possible to assimilate the layers of the printed vault to the rows of bricks in the masonry vault.

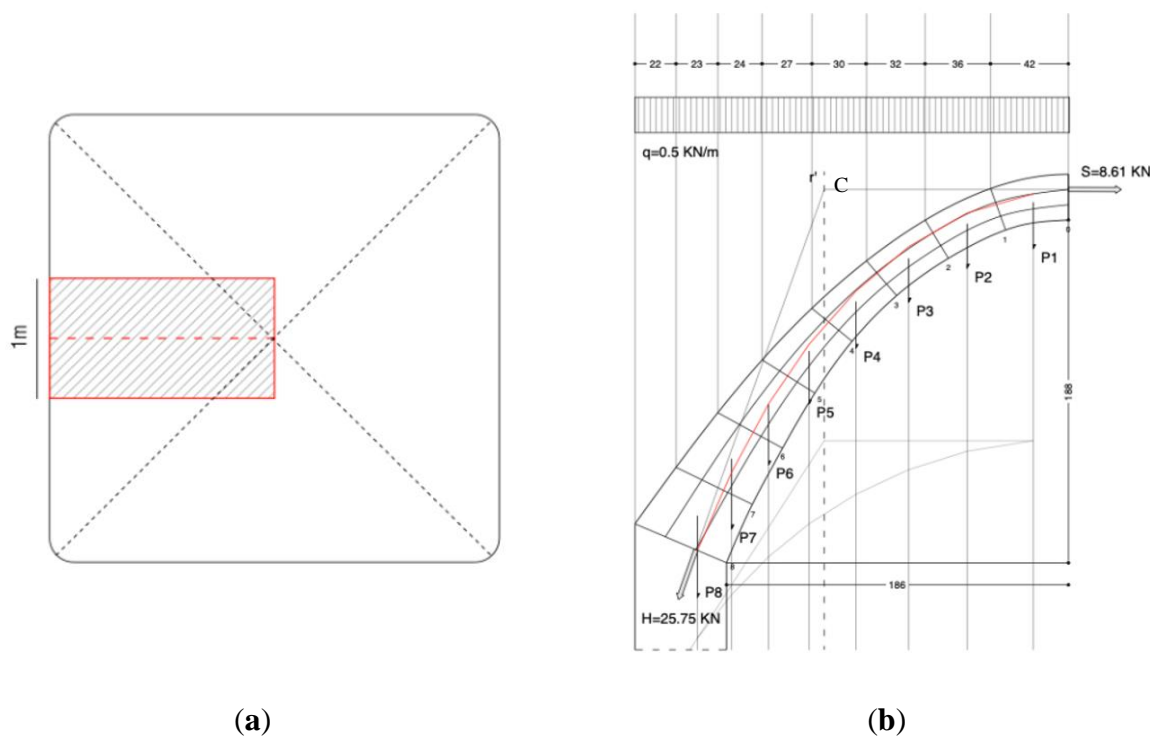


**Figure 5.** (a) Study band for the pressure curve; (b) Verification of the pressure curve passing through the middle third of the section.

**Table 3.** Weight of individual segments, load analysis carried out at the ULS.

Segment	Weight
1	2.51 kN
2	2.38 kN
3	2.37 kN
4	2.54 kN
5	2.87 kN
6	3.31 kN
7	3.82 kN
8	4.45 kN

Proceed to verify the bending stress in the key.

Design compression stress:

$$F_d = \frac{F'_c}{\gamma} = \frac{0.62}{2} = 0.31 \text{ MPa}, \quad (1)$$

Applied stress:

$$F_e = \frac{2 \cdot S}{b \cdot s} = \frac{2 \cdot 8610}{1000 \cdot 250} = 0.069 \text{ MPa}, \quad (2)$$

With:

- $\gamma$ = Safety factor;
- $b$ = Length of the block
- $s$ = Height of the block

The verification is passed as  $F_e < F_d$

Proceed to verify the bending and shear stresses at the impost. For bending:

Orthogonal force component at the impost:

$$H' = 25.70KN, \quad (3)$$

Applied stress:

$$F_e = \frac{2 \cdot H'}{b \cdot s} = \frac{2 \cdot 25700}{1000 \cdot 540} = 0.095MPa, \quad (4)$$

The verification is passed as  $F_e < F_d$

For shear verification:

Average normal stress on the section:

$$\bar{\sigma}_n = \frac{H'}{b \cdot s} = \frac{25700}{1000 \cdot 540} = 0.047MPa, \quad (5)$$

Maximum shear with normal force:

$$F_{vk} = F'_{vk0} + 0.4 \cdot \bar{\sigma}_n = 0.26MPa, \quad (6)$$

Design shear stress:

$$F_{vd} = \frac{F_{vk}}{\gamma} = \frac{0.26}{2} = 0.13MPa, \quad (7)$$

Parallel force component at the impost:

$$H'' = 1.6KN, \quad (8)$$

Applied shear:

$$F_{ve} = \frac{H''}{b \cdot s} = \frac{1600}{1000 \cdot 540} = 0.003MPa, \quad (9)$$

The verification is passed as  $F_{ve} < F_{vd}$

The same procedure was used for the verification of the 9 sqm and 4 sqm blocks, but only the final results are reported.

Table 4. 9 sqm block verifications.

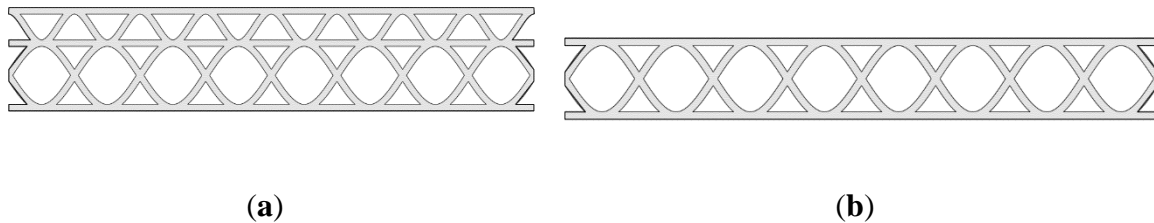
Pressure curve	Bending under compression (Keystone) [MPa]	Bending under compression (Impost) [MPa]	Shear (Impost) [MPa]
Contained in the middle third	0.057<0.31	0.076<0.31	0.002<0.13

Table 5. 4 sqm block verifications.

Pressure curve	Bending under compression (Keystone) [MPa]	Bending under compression (Impost) [MPa]	Shear (Impost) [MPa]
Contained in the middle third	0.038<0.31	0.052<0.31	0.002<0.13

### 2.2.3. Wall

Two different types of walls were defined, perimeter wall (Figure 6a) and internal wall (Figure 6b). The first divides a covered space from an open space, supporting the weight of a single roof, the second divides two covered spaces and supports the weight of two roofs.



**Figure 6.** (a) Perimeter wall; (b) Internal wall.

The first case considered is that where the wall supports the load of the two larger coverings, i.e., the internal wall between two 12 sqm modules, evaluating the load of the covering uniformly distributed in length. This structural design is based on the procedure of the paper [16].

The structural design is carried out following the limit state method, it is possible to define the design resistance as:

$$P_d = \frac{P}{\gamma}, \quad (10)$$

with:

- $P_d$ = Design resistance;
- $P$ = Maximum compression load;
- $\gamma$ = Safety factor taken as 2.

To define the compressive strength of the wall, it is first necessary to design the type of infill resistant to vertical loads. The geometry of the wall section (Figure 7a) was studied by formulating an algorithm in Grasshopper.

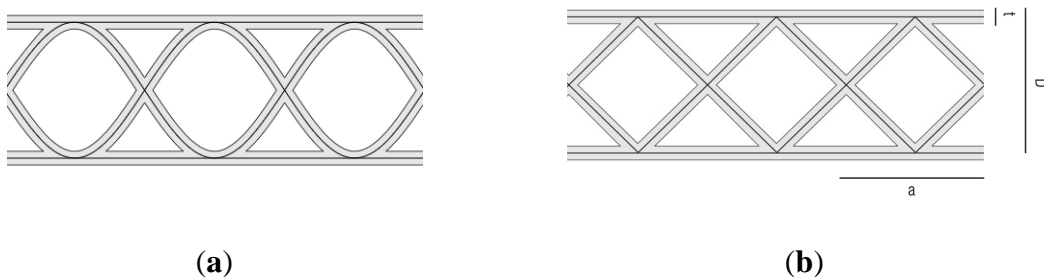


**Figure 7.** (a) Actual wall section; (b) Analyzed geometric simplification.

Highlighting how the infill step (a) is equal to the thickness (D) of the wall, in this way the entire section can be described with only two parameters (D) and (t) nozzle thickness.

For the evaluation of the mechanical compressive strength of the wall, the simplified resistant section (Figure 7b) was studied. We need the geometric characteristics of the section: Area (A) and Moment of Inertia (I). These quantities are studied on the simplified section (Figure 7b), dependent on the two parameters (D) and (t). For the evaluation of these characteristics, a wall section with a length (L) of 1000mm and a height (H) of 2200mm was studied.

Wall path length:

$$L_i = \frac{L}{D} \cdot D \cdot \sqrt{2} + L, \quad (11)$$

Moment of inertia of internal infill:

$$I_{ob} = \frac{\left(\frac{2t}{\sqrt{2}}\right) \cdot \left(\frac{D}{2}\right)^3}{12} + \left(\frac{D}{4}\right)^2 \cdot D \cdot \frac{\sqrt{2}}{2} \cdot t, \quad (12)$$

Moment of inertia of external shell:

$$I_{or} = \frac{t^3 \cdot L}{12} + t \cdot L \cdot \left(\frac{D}{2}\right)^2, \quad (13)$$

Total moment of inertia:

$$I_{Tot} = I_{ob} \cdot 4 \cdot \frac{L}{D} + I_{or} \cdot 2, \quad (14)$$

The vertical loads were evaluated in the study of the roof; in this case, the stresses of the 12 sqm block roof were used.

Considered loads:

- Roof weight  $P_r = 25.70$  KN;
- Wall weight  $P_w = 1.3 \cdot 18 \cdot 10^{-9} \cdot (A \cdot 2000 + D \cdot L \cdot 200)$
- Total weight  $P_{tot} = P_w + 2 \cdot P_r$ .

The maximum compressive strength of the wall is the lesser of the characteristic compressive strength of the material and the maximum stress due to local instability.

Maximum compressive strength of the wall:

$$\sigma_{c,max} = \min(f'_c; \sigma_{Buck,loc}) = \min(0.62; \sigma_{Buck,loc}), \quad (15)$$

The first has already been determined by axial compression tests, and it is 0.62 MPa (Table 2), while the second was evaluated by studying the local instability of the individual elements that make the wall:

Effective buckling length:

$$L_m = 2000 \text{ mm}, \quad (16)$$

Number of bucklings over the length:

$$m = \frac{L_m}{D}, \quad (17)$$

Instability coefficient [19]:

$$k_{cr} = \left( \frac{(m \cdot D)}{L_m} + \frac{L_m}{(m \cdot D)} \right)^2, \quad (18)$$

Maximum stress for local instability of a simply supported plate [19]:

$$\sigma_{Buck,loc} = k_{cr} \cdot \frac{(\pi^2 \cdot E)}{12 \cdot (1 - \nu^2)} \cdot \left(\frac{t}{D}\right)^2 \quad (19)$$

Finally we can define the maximum stress value within the section, studied as a column subject to eccentric load with the possibility of global instability.

Maximum compressive stress:

$$\sigma_{c,\max} = P \cdot \left( \frac{1}{A} + \frac{e \cdot c}{I_{\text{Tot}}} \sec \left( \frac{\pi}{2} \cdot \sqrt{\frac{P}{P_{\text{Buck, glob}}}} \right) \right), \quad (20)$$

with:

- Distance between the mid-axis of the wall and the outermost tensioned fiber  $c = \frac{D}{2}$  ;
- Maximum load for global instability  $P_{\text{Buck, glob}} = \frac{\pi^2 \cdot E \cdot I}{L_m^2}$  ;
- Total eccentricity of vertical loads  $e = \frac{\sum P_i \cdot e_i}{P_{\text{Tot}}}$  ;
- Eccentricity of the wall's own weight  $e_m = 0.05D$  ;

The maximum load is evaluated by solving equation (20) for  $P$ . The geometry of the wall section is defined by the variables  $D$  wall thickness and  $t$  nozzle size. It is possible to optimize these dimensions to have the least amount of printed material and exactly the capacity needed to withstand the applied stresses. We define  $u$ , utilization coefficient:

$$u = \frac{P_{\text{tot}}}{P_d}, \quad (21)$$

$u$  is the ratio between the load applied on the wall ( $P_{\text{tot}}$ ) and the design resistance of the wall ( $P_d$ ). The ratio depends only on  $t$  and  $D$ , so it is possible to calculate the values of the pair ( $t, D$ ) for which  $u=1$  and  $P_d=P_{\text{tot}}$

The study for the perimeter wall was carried out similarly, considering a perimeter wall of the 12 sqm block, a halved vertical load and taking into account the eccentricity of the vertical load of the overlying vault.

$$e = \frac{\sum P_i \cdot e_i}{P_{\text{Tot}}}, \quad (22)$$

with:

- Eccentricity of the wall weight  $e_m = 0.05D$ ;
- Eccentricity of the roof weight  $e_c = 0.16D$ ;

When calculating the value of the maximum vertical load, the internal stress of the wall section due to the moment generated by the horizontal force of the roof was also evaluated.

$$\sigma_{c,\max} = P \cdot \left( \frac{1}{A} + \frac{e \cdot c}{I_{\text{Tot}}} \sec \left( \frac{\pi}{2} \cdot \sqrt{\frac{P}{P_{\text{Inst, glob}}}} \right) \right) + \frac{M}{I_{\text{Tot}}} \cdot c, \quad (23)$$

with:

- $M = S \cdot L_m$

### 3. Results

#### 3.1. Structural Design Results

The pairs ( $t, D$ ) were found by writing a program in python, finding all the values of  $u$  from the possible combinations of ( $t, D$ ) and plotting the graph of the points of interest where  $u=1$ .

The obtained graph (Figure 8) represents the domain of sections with adequate capacity for the internal wall. The curve  $u=1$  follows two different trajectories depending on whether it is in the region of compact or slender sections. In the region of compact sections, the maximum stress is the maximum compressive strength of the material (Table 2), while in the region of slender sections, the maximum strength is the maximum stress for local instability (19). We can observe how the domain has a minimum point, where the pairs ( $t, D$ ) results in equal values of maximum stress for local instabilities

and compressive strength of the material. The minimum coincides with the optimal point, where we have adequate strength to withstand the loads with the least amount of material used.

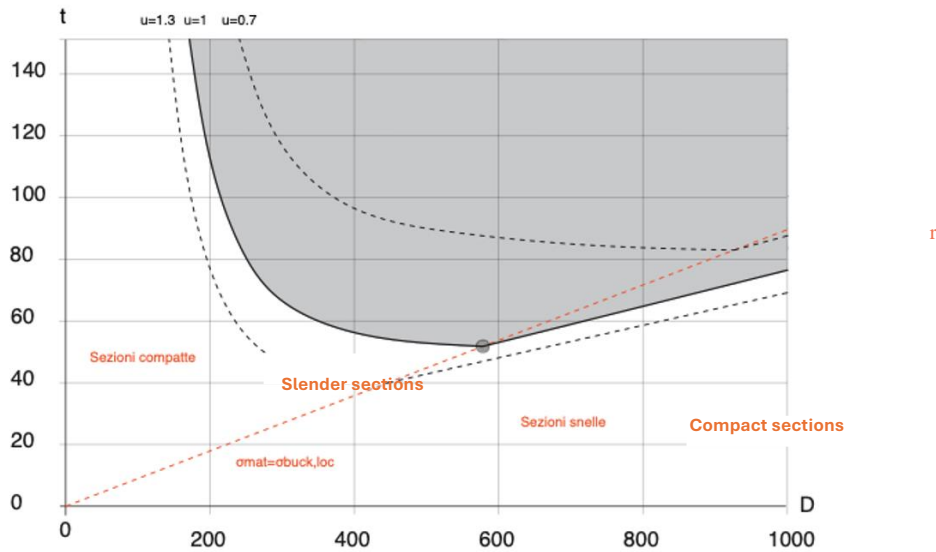


**Figure 8.** Graph of the resistance domain of the internal wall section.

The graph just obtained was then compared with the one resulting from the preliminary design of the perimeter wall derived in a similar manner (Figure 9). In the latter, we notice that, although the value of the vertical load is halved compared to the intermediate case, the presence of the horizontal force of the roof leads to having optimal values of  $t$  and  $D$  greater than those of the internal wall.

The line  $r$  is given by all pairs  $(t,D)$  for which  $\sigma_{inst,loc}=0.62$  MPa, found using the instability formula for simply supported plates (19). The values obtained were compared with the values obtained from the simulations carried out in ABAQUS.

Two simulations were carried out (Figure 10) to evaluate the instability values obtained on wall sections with a length and height of 2000 mm. The parameters  $(t)$  and  $(D)$  used for the modeling were taken from the line  $r$  drawn in the graph (Figure 8): in the first case  $D=575$  mm and  $t=53$  mm, in the second case  $D=1000$  mm and  $t=90$  mm. In both cases, the maximum stress values for instability coincide with the maximum compressive stress of the material, validating the values obtained through equation (19).

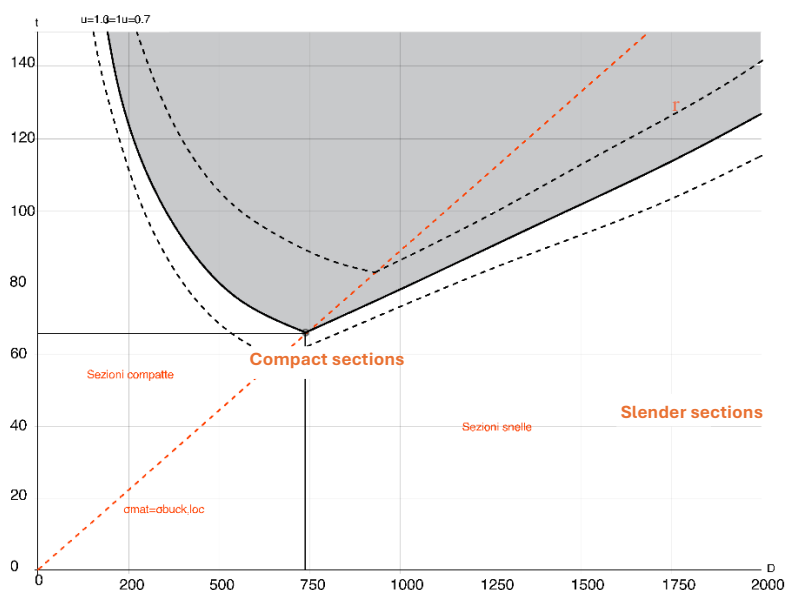


**Figure 9.** Graph of the resistance domain of the perimeter wall section.

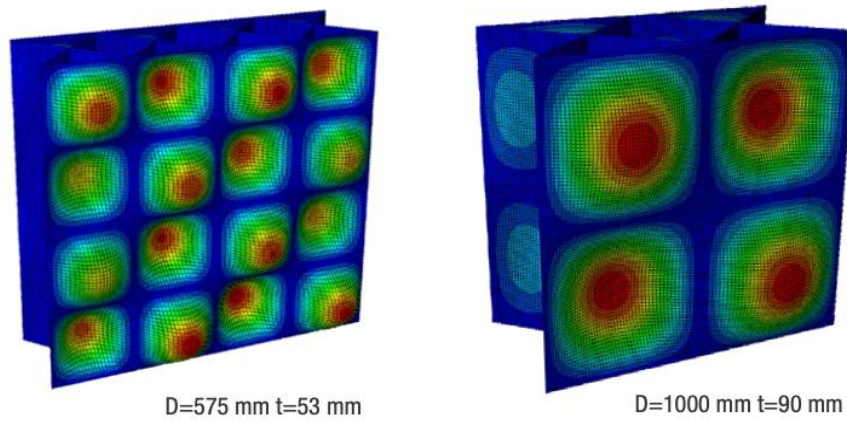


**Figure 10.** Simulation results in ABAQUS.

The wall project was concluded by verifying that the resultant force between the roof load and the wall weight was contained within the middle third of the wall thickness at the base for both perimeter and internal walls (Figure 11), providing for a tapered outer layer capable of absorbing the horizontal thrusts of the roof, in the case of a perimeter wall (Figure 12).

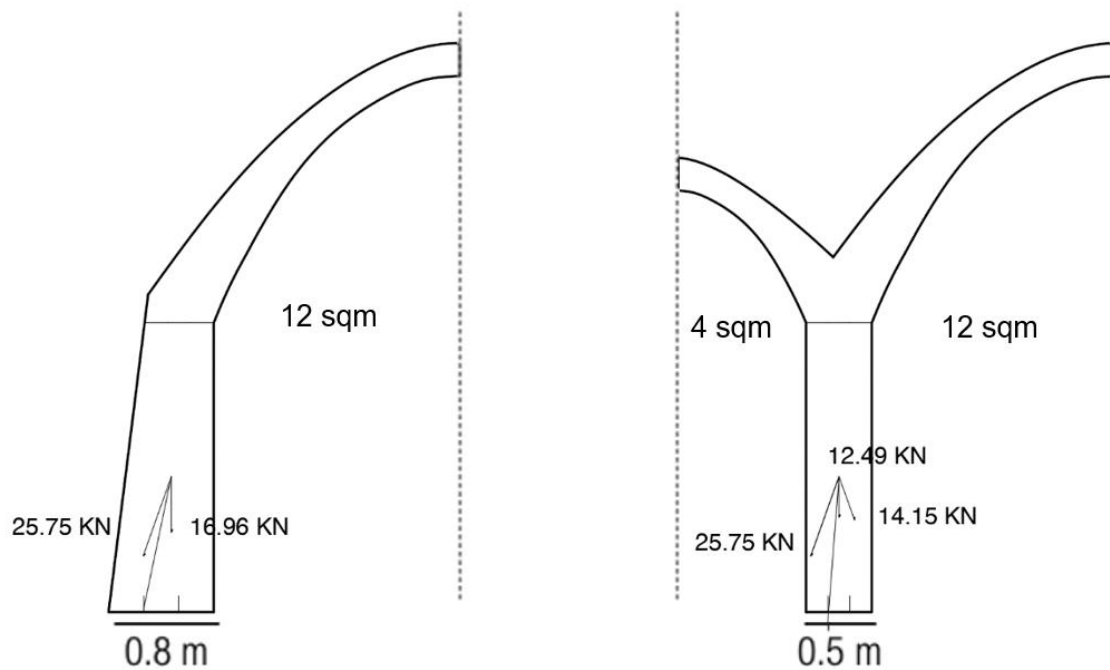


**Figure 11.** Verification of the force passage within the middle third of the wall base.

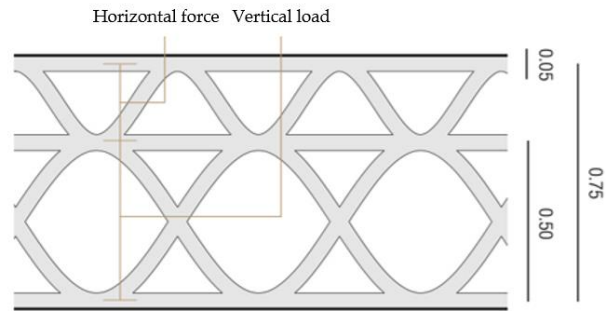


**Figure 12.** Final infill definition for perimeter wall.

### 3.2. The Architectural Project

The project is located in the eastern outskirts of Niamey, in Niger, a North African state that is among the largest in terms of population growth [20]. The urban context is very dense and characterized by the presence of informal housing, the compounds (Figure 13), a large-scale residential typology, where we find self-built blocks, with few openings to the outside, built very close together and enclosed by a perimeter wall. The demand for modernization of the construction techniques used so far locally is leading to a loss of local identities, as imported materials are adopted, resulting in solutions that are not suitable for the context in which they are used.

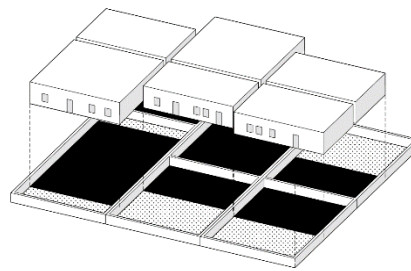


**Figure 13.** Compound layout.

The intervention idea is summarized in six points and is based on the study of the traditional local way of living, characterized by a strong presence of community spaces:

- Starting from the average size of a current dwelling (Figure 14a);
- Increasing the density by creating two units where previously there was one unit in the same area (Figure 14b);
- The individual dwellings are divided into functional modules (Figure 14c);
- The modules are then arranged to create the new house (Figure 14d);
- The housing units are aggregated to create a settlement (Figure 14e);
- The system is completed with the insertion of central community spaces (Figure 14f).

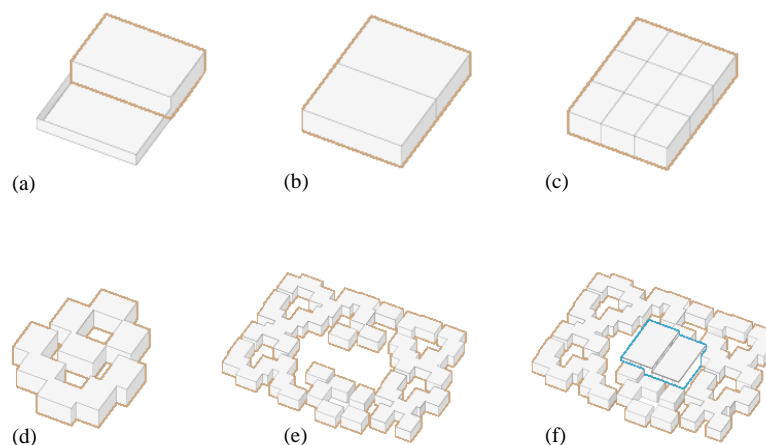


**Figure 14.** Settlement concept: (a) Current dwellings, (b) Increased density, (c) Module division, (d) Patio openings, (e) Aggregation, (f) Insertion of common spaces.

The project consists of ten dwellings that enclose a central common space (Figure 15). The plan takes up the idea of a fenced compound. The design is based on the definition and arrangement of individual modules that represent the rooms fulfilling the functions of living. The jagged arrangement of the modules allows for the creation of residences where we find the alternation of covered spaces and shaded patios, as in extremely hot climates it is essential to be able to carry out part of the daily activities outdoors.

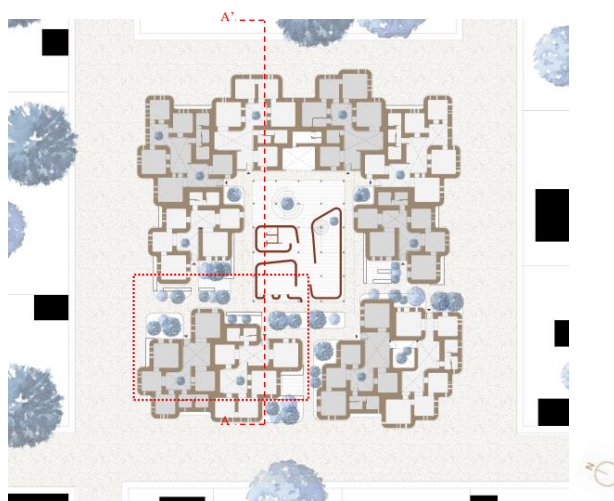


**Figure 15.** Ground floor plan.

Regarding the relationship with the context: the dwellings have small heights, remaining on a single floor, not overshadowing the surroundings. The only block of greater height is the central collective building arranged on two levels. Specifically, this central block is not made of load-bearing earth; instead, the walls printed with earth are positioned in a regular grid of wooden pillars that support the floors (Figure 16). Although this block has two floors, it has a much lighter character compared to the surrounding buildings.

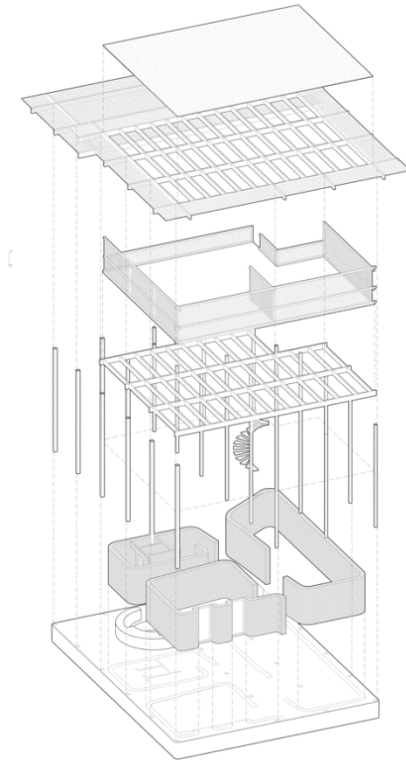


**Figure 16.** Exploded view of the central block of common spaces.

All housing units follow the same design logic (Figure 17): there is a division between the blocks of the living area and the blocks of the sleeping area, the latter being separated from the former by a study area that functions as a filter. The rooms are arranged around internal courtyards where there are vegetation, shared spaces, kitchens, and areas for outdoor dining. Each unit has its own covered kitchen. The outdoor kitchens are built adjacent to the service blocks to minimize the layout of the systems. It is possible to enter the homes through the internal paths of the aggregation and not from the street front.

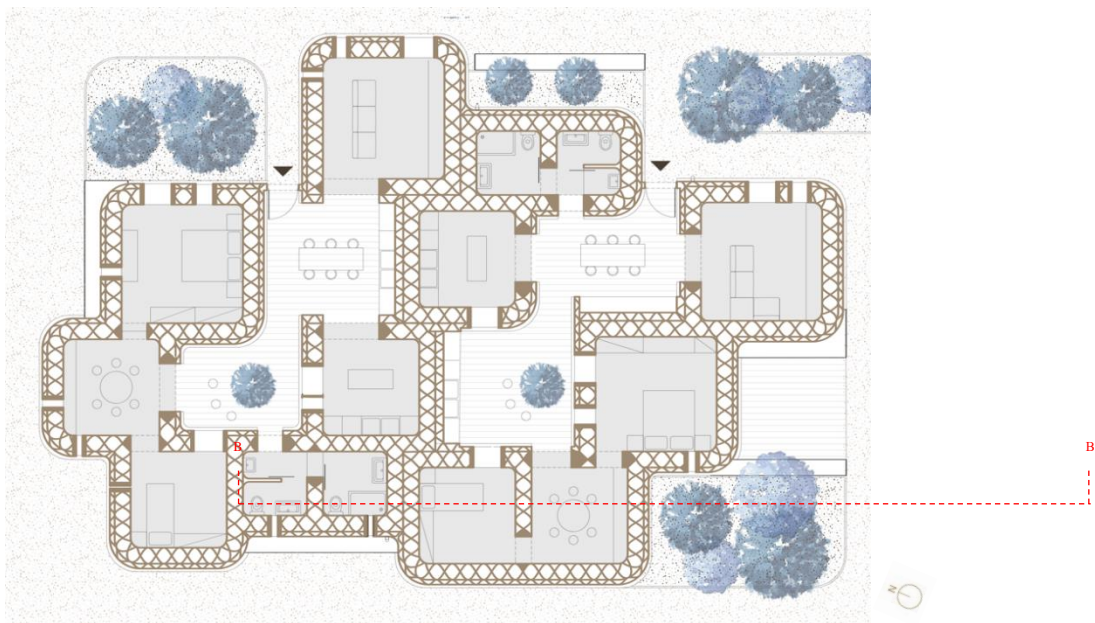


**Figure 17.** Detail of the housing block, highlighted in Figure 15.

The project focuses on developing a settlement idea that is not limited to the single housing unit, which is the private domain of the family, but can be defined as an aggregative system of parts, where we find a constant dialogue between private and common spaces, between the individual and the community. The planned environments have different degrees of privacy:

- Those of an individual nature, such as bedrooms and bathrooms;
- Family spaces, such as the living room, kitchen, and patios;
- Those of the community.

The exteriors gain fundamental importance and influence the design of the covered spaces; in fact, all the covered rooms are arranged around an open core. This occurs on two scales, the first at the level of the dwelling and the second at the level of aggregation.

From the elevation (Figure 18) and the section (Figure 19), we can read the elevation configuration of the blocks. The roof base level is the same for all the units regardless of size, but the roof height varies with the plan size of the module. This allows for a dual characterization of living spaces, the first being covered – open and the second based on different internal heights. We can also observe the difference in the perforations that open onto the street fronts and those inside: both are designed according to the same principle, that is, to be made directly during the printing phase. However, the former are small and very dense, while the latter are fewer in number and larger in size. Regarding the wall, we see how it is connected in the foundation with channels that allow for ventilation (Figure 20), maintaining proper internal comfort and preventing overheating.



**Figure 18.** Southwest elevation.

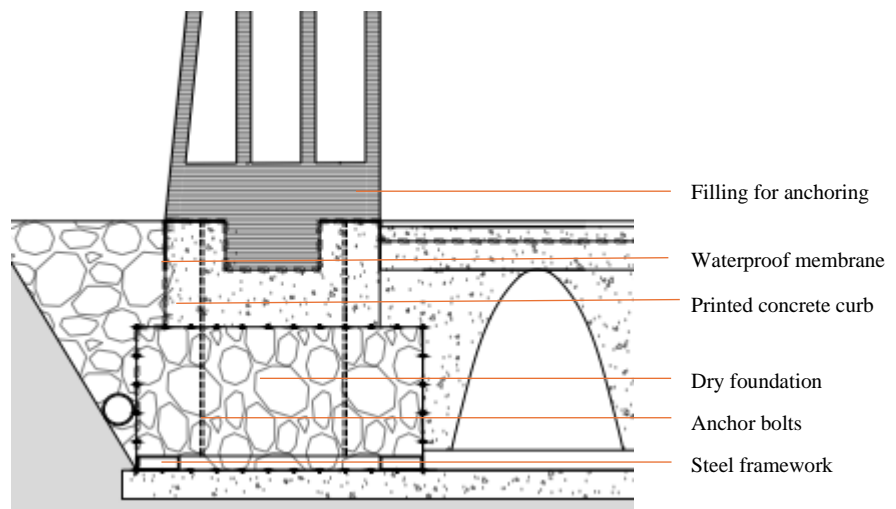


**Figure 19.** Section A-A' (Figure 15).

As for the foundations of the houses, an effort was made to reduce the amount of cement used by employing dry foundations (Figure 21). These foundations are made of welded wire mesh gabions filled with gravel, with a metal frame attached to the bottom panel to which the anchor bolts are connected [21]. The earthen wall is separated from the foundation by a concrete printed curb, connected to the foundation by anchor bolts. The upper end of the curb is shaped with a notch, into which the earthen wall fits, making the wall-foundation system united. The printing of the wall starts above the ground level and is separated from the curb with a waterproof membrane to prevent contact with the soil and potential water infiltration. The floor slab is in contact with the ground; however, an aerated crawl space is printed in concrete to allow air circulation within the wall.



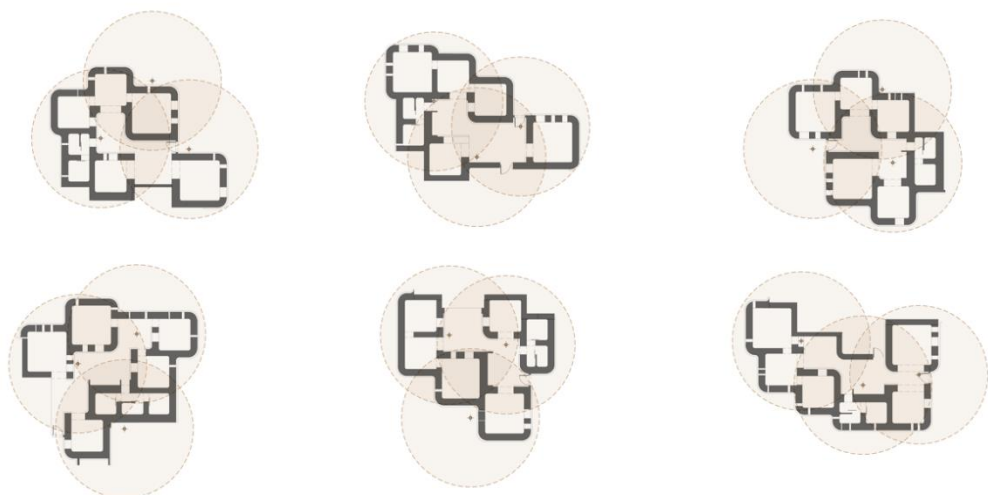
**Figure 20.** Section B-B' (Figure 17) with air recirculation.



**Figure 21.** Detail of perimeter wall foundation.

It should be emphasized that the realization of the settlement through 3D printing allows the possibility of customizing functional blocks according to the needs of the inhabitants, opening up new possibilities for participatory design, and adapting the project as best as possible to the needs of the community. Given the extreme flexibility of the construction process, it should be specified that the one shown in Figure 15 is only one possible aggregation of the units, but the same design process could be replicated to define linear, terraced, or block typologies.

The project is conceived with a view to programmed expansion. As for the houses, each one is built by 3 robotic arms that operate together (Figure 22). This is an evolution of the simultaneous extrusion arm technology, first experimented with in the construction of the Tecla prototype. The positioning of the arms is facilitated by the presence of internal courtyards, which are utilized during the construction phases. In this way, the walls and roofs are raised simultaneously, ensuring proper bonding. Each house is therefore independent from the adjacent ones so that they can be built in distinct temporal phases. A planned expansion of the aggregate is therefore foreseen in 4 temporal phases (Figure 23), starting from phase 1 where we see the construction of the central block, so that it can be immediately used by the inhabitants of the nearby compounds. Subsequently, in phases 2 to 4, the peripheral dwellings will be executed.



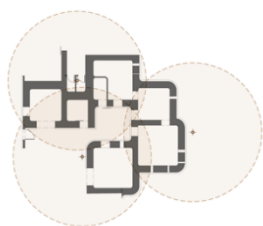


**Figure 22.** Positioning of arms for housing printing.

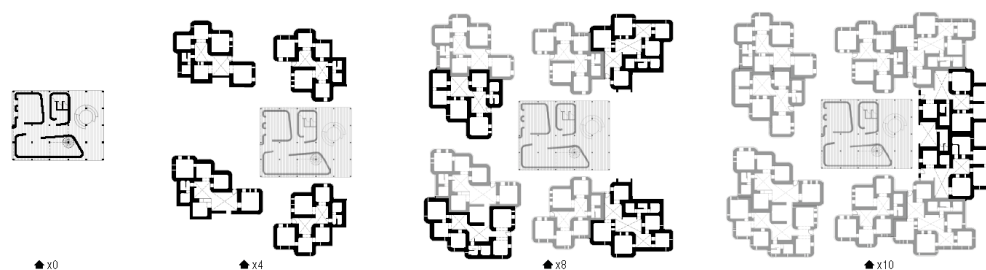


**Figure 23.** Settlement printing phases: (a) Common spaces, (b) x4 dwellings, (c) x8 dwellings, (d) x10 dwellings.

#### 4. Conclusions

The studied strategy allows for the design and sizing of the system's construction elements so that they can meet both structural and spatial requirements, maximizing the automation of the construction process.

The designed system, in fact, based on the use of robotic arms that deposit the earthen compound in inclined layers, defines an on-site construction strategy with sustainable materials, where it is possible to use the printer as the main construction tool, ensuring the complete printability of the entire building.

This entails numerous design advantages:

- **Speed of construction:** the estimated time, considering the amount of material printed for the construction of a house and the printing speed of a modern robotic arm (about  $6 \text{ dcm}^3/\text{min}$ ) [22], is approximately 70 hours using 3 robotic arms simultaneously.
- **Scalability:** The houses are completely autonomous, allowing the entire settlement to be realized in phases, so that the constructed spaces can be used immediately;
- **Design flexibility:** the defined system is capable of varying based on the functional requirements, increasing the customization of built environments. The project variation occurs on two scales: the module scale (the definition of the choice of the rooms depends on the needs of the inhabitants); and the aggregation scale (the arrangement of the modules can vary based on the urban context, defining different types of housing). Customizations do not increase the construction time of individual houses;
- **Sustainability:** the printing compound is entirely extractable and manufacturable on-site, reducing pollution due to the transportation and production of construction materials. Moreover, being a natural compound, it is also easily disposable. The earthen mixture is used for most of the construction, with the only exception being the foundation system (where a dry technology was adopted to minimize the use of concrete to just the base course of the walls) and the central wooden block;
- **Computational workflow:** 3D printing allows the application of modern parametric design systems to one of the oldest building materials, the earth. This allows for the study and realization of forms optimized based on various needs: structural, thermal, or spatial. The design is therefore based on initial parameters and guided by computational tools. In particular, in the case study,

the geometries of the modules were optimized to automate the construction process, while the definition of the wall infill was made to withstand the thrusts of the roof.

## 5. Future Developments

- Variation of wall strength with the variation of infill: defining different typologies of the wall infill in order to change it according to the different load conditions on the wall.
- Possibility of lightening the roof: designing an infill typology for the roof in order to lower the impact of the vault on the walls. This should greatly improve the design quality of the module in different ways: first, lower the amount of earthen mixture used to print one module, resulting in thinner walls and a better utilization of the space; second, further decreasing the printing time for each housing unit.
- Future scenarios of participatory design: the vision for the project is designing a housing system that can be easily customized by the people that will live it. 3D printing technology allows to have a direct connection between the machine and the software. A step forward to the current project would be to understand what other types of functional modules can be designed and how each one of them can be customized by the future owner, creating a catalog. This also implies developing an interface where people can design and request their custom houses based on their needs.

## References

1. Ratti, C., & Claudel, M. (2015). Open source architecture (pp. 18-22). London: Thames & Hudson.
2. Paparella, G., & Percoco, M. (2022, June). 3D Printing for Housing. Recurring Architectural Themes. In International Conference on Technological Imagination in the Green and Digital Transition (pp. 309-319). Cham: Springer International Publishing.
3. Skinner, B., & Lalit, R. (2023, January 17). Shares With Concrete, Less Is More. Demand changes can drive the future of zero-carbon concrete
4. Global cement and concrete association. (n.d.). The GCCA 2050 Cement and Concrete Industry Roadmap for Net Zero Concrete CONCRETE ROADMAP OVERVIEW DOCUMENT GCCA Concrete Future-Roadmap Overview..
5. United Nations Environment Programme (2022). (2022). *2022 Global Status Report for Buildings and Construction: Towards a Zero-emission, Efficient and Resilient Buildings and Construction Sector*. www.globalabc.org.
6. Gallipoli, D., Bruno, A. W., Perlot, C., & Mendes, J. (2017). A geotechnical perspective of raw earth building. In Acta Geotechnica (Vol. 12, Issue 3, pp. 463-478). Springer Verlag. <https://doi.org/10.1007/s11440-016-0521-1>
7. Santamouris, M., & Kolokotsa, D. (2013). Passive cooling dissipation techniques for buildings and other structures: The state of the art. In Energy and Buildings (Vol. 57, pp. 74-94). <https://doi.org/10.1016/j.enbuild.2012.11.002>
8. Guamán-Rivera, R., Martínez-Rocamora, A., García-Alvarado, R., Muñoz-Sanguinetti, C., González-Böhme, L. F., & Auat-Cheein, F. (2022). Recent developments and challenges of 3D-printed construction: A review of research fronts. Buildings, 12(2), 229.
9. Chiusoli, A. (2018, September 29). La prima Casa Stampata in 3D generata con la Terra | Gaia | Stampanti 3D. WASP. <https://www.3dwasp.com/casa-stampata-in-3d-gaia/> accessed online 02/08/2024.
10. Mario Cucinella Architects. (2021). Mario Cucinella Architects. Mario Cucinella Architects. Retrieved August 2, 2024, from <https://www.mcarchitects.it/en/projects/tecla-technology-and-clay>
11. Civera, G. TOVA is Spain's first 3D printed building using raw earth (3dwasp.com), accessed online 03/08/2024.
12. Wasp, 3D printed house\_Gaia\_WASP\_overall view, Gaia press release. Press Kit Gaia 3d printed house - Dropbox, accessed online 03/08/2024.
13. Corrazza, I. Dettaglio: Struttura in terra stampata in 3D del prototipo TECLA, Ravenna | Archello, accessed online 03/08/2024.
14. Adobe Dome & Nubian Vault – Canelo Project, accessed online 03/08/2024.
15. Carneau, P., Mesnil, R., Roussel, N., & Baverel, O. (2019). An exploration of 3d printing design space inspired by masonry. <https://doi.org/10.5281/zenodo.3563672i>
16. Vaculik, J., Author, F., Gomaa, M., Soebarto, V., Griffith, M., & Jabi, W. (n.d.). Construction and Building Materials Feasibility of 3DP Cob Walls Under Compression Loads in Low-Rise Construction 3 4 Mohamed Gomaa ae.

17. Sangma, S., & Tripura, D. D. (2021). Compressive and shear strength of cob wallettes reinforced with bamboo and steel mesh. *Proceedings of the Institution of Civil Engineers: Structures and Buildings*, 176(9), 710–724. <https://doi.org/10.1680/jstbu.21.00086>
18. Ferretti, E., Moretti, M., Chiusoli, A., Naldoni, L., de Fabritiis, F., & Visonà, M. (2022). Mechanical Properties of a 3D-Printed Wall Segment Made with an Earthen Mixture. *Materials*, 15(2). <https://doi.org/10.3390/ma15020438>
19. Clarin, M. (n.d.). Plate Buckling Resistance - Patch Loading of Longitudinally Stiffened Webs and Local Buckling.
20. Maja, M. M., & Ayano, S. F. (2021). The impact of population growth on natural resources and farmers' capacity to adapt to climate change in low-income countries. *Earth Systems and Environment*, 5(2), 271–283.
21. Simeoni, L., Ferro, E., Molinari, M., Gerola, M., Gajo, A., Polastri, A., Fanti, R., Rossi, S., & Benedetti, L. (n.d.). Fondazioni a secco per edifici in legno AUTORI.
22. Apis Cor. (n.d.). Construction can be fast, environmentally friendly, and affordable if we entrust all the complex work to smart machines.

**Disclaimer/Publisher's Note:** The statements, opinions and data contained in all publications are solely those of the individual author(s) and contributor(s) and not of MDPI and/or the editor(s). MDPI and/or the editor(s) disclaim responsibility for any injury to people or property resulting from any ideas, methods, instructions or products referred to in the content.